microbial biotechnology

Microbial Biotechnology (2011) **4**(2), 263–274 doi:10.1111/j.1751-7915.2010.00237.x

Forkhead-associated proteins genetically linked to the serine/threonine kinase PknB regulate carbon flux towards antibiotic biosynthesis in *Streptomyces coelicolor*

Greg Jones, Ricardo Del Sol, Ed Dudley and Paul Dyson*

Institute of Life Science, Swansea University, Singleton Park, Swansea SA2 8PP, UK.

Summary

To date, the function of only two of the 34 predicted serine/threonine protein kinases (STPKs) of *Streptomyces coelicolor* has been described. Here we report functional analysis of *pknB* and two linked genes, *fhaAB*, encoding forkhead-associated (FHA) domain proteins that are part of a highly conserved gene locus in actinobacteria. In contrast to the homologous gene of *Mycobacterium tuberculosis*, *pknB* in *S. coelicolor* is not essential and has no apparent role in defining cell shape. Phosphorylation of recombinant forms of both the full-length protein and N-terminal kinase domain suggest that PknB-mediated signalling in *S. coelicolor* may be modulated by another factor(s). FhaAB are candidate interacting partners of PknB and loss of their function resulted in deregulation of central carbon metabolism, with carbon flux diverted to synthesis of the antibiotic actinorhodin. The substrate hyphae of the *fhaAB* mutant also exhibited an unusual cording morphology. The results indicate that inactivation of FHA 'brake' proteins can potentially amplify the function of STPKs and, in this case, provide a means to overproduce antibiotics.

Introduction

Streptomyces are unusual Gram-positive soil bacteria that grow as a mycelium of branching hyphae. They have very versatile metabolisms and are especially renowned for the diversity of secondary metabolites they can synthesize, encompassing a wide range of medically important natural products including many different antibiotics. The typical streptomycete life cycle involves a switch from exponential growth of the substrate mycelium to development of specialized spore-bearing aerial hyphae. Broadly coincident with this switch is a transition from primary metabolism to allow synthesis of secondary metabolites. This reprogramming of growth and metabolism is determined by a variety of stimuli, both environmental and inherent, that affect expression of complex regulatory networks involving pleiotropic and stress-related factors (Bibb, 1996; Chater, 2001). This is probably best exemplified in the model streptomycete, *S. coelicolor*, and recent transcriptomic and proteomic data indicate the large extent by which patterns of global gene expression are modified in order to reprogram growth and metabolism (Hesketh *et al*., 2007a,b; Nieselt *et al*., 2010).

The complexity of the life cycle and the need, as free-living organisms, to adapt to a wide range of environmental conditions probably explains the large and diverse regulatory capacity of a typical streptomycete genome. Twelve per cent of the 8.7 Mb *S. coelicolor* genome is predicted to have regulatory function, with, for example, 65 different sigma factors, 101 sensor histidine kinases and 80 response regulators (Bentley *et al*., 2002; Hutchings *et al*., 2004). In addition, there are 34 predicted serine/threonine protein kinases (STPKs) (Petrickova and Petricek, 2003). Of these STPKs, only two have been investigated in any detail, demonstrating that they have roles in regulating development and antibiotic production. RamC (SCO6681) is a membrane protein with an N-terminal cytoplasmic kinase domain (although no kinase activity has been reported) and is encoded as part of the *ramCSAB* operon, the source of the hydrophobic secreted oligopeptide SapB that functions as a surfactant to allow aerial hyphae to escape the aqueous milieu of the substrate colony (Kodani *et al*., 2004). Via its C-terminal domain, RamC is proposed to function as a lantibiotic synthetase in the synthesis of SapB. The second and better characterized STPK is AfsK (SCO4233) (Umeyama *et al*., 2002). This is a global regulator of secondary metabolism in *S. coelicolor* and of development in *S. griseus*. AfsK autophosphorylates and can subsequently phosphorylate the pleiotropic transcription factor AfsR.

Received 6 October, 2010; accepted 27 October, 2010. *For correspondence. E-mail p.j.dyson@swansea.ac.uk; Tel. (+44) 1792 295667; Fax (+44) 1792 602147.

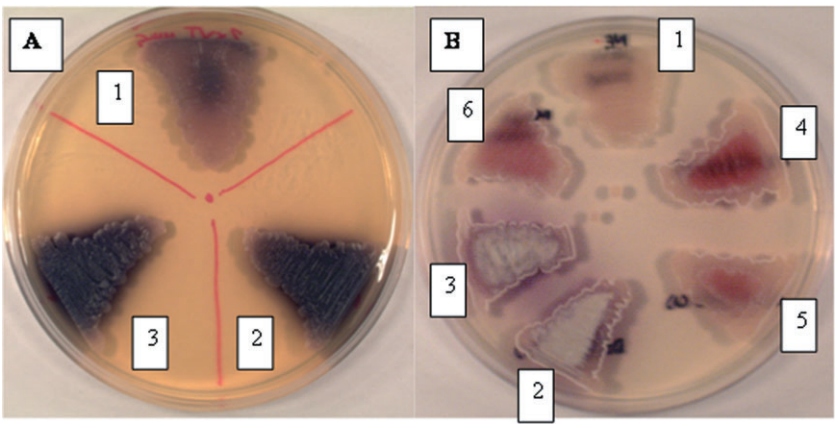

Fig. 1. Increased antibiotic production and precocious aerial development of the *pknB* mutant.
A. Parental strain M145 (1) and two independently isolated *pknB* mutants (2 and 3) were grown on 2xYT media for 72 h.
B. The same strains were grown on NE medium for 72 h together with the complemented mutants containing plasmid pSC3848 (4 and 5) and M145 containing empty vector pSH152.

AksK activation, and hence AfsR phosphorylation, is blocked by binding of KbpA, encoded by the gene immediately upstream of *afsK*, to the kinase domain of AfsK. However, there is evidence for promiscuous phosphorylation of AfsR by two other relatively uncharacterized STPKs: PkaG (SCO4487) and AfsL (SCO4377) (Horinouchi, 2003).

Other related actinobacteria that are unicellular, with smaller genomes and arguably less complex life cycles, possess a reduced regulatory capacity with, for example, 13 and 4 STPKs encoded by the genomes of *Mycobacterium tuberculosis* and *Corynebacterium glutamicum* respectively (Cole *et al*., 1998; Fiuza *et al*., 2008). An STPK shared by all these different bacteria is PknB, encoded by a gene in a highly conserved locus that includes the essential *rodA* gene encoding a polytopic membrane protein involved in peptidoglycan synthesis during growth (Mistry *et al*., 2008). *pknB* is essential in *M. tuberculosis* and manipulation of its expression alters cell shape (Kang *et al*., 2005). In this paper, we address the function of *pknB* and linked genes encoding two forkhead-associated domain proteins in *S. coelicolor*. We demonstrate that inactivation of the latter two genes has a profound effect on the transition between primary and secondary metabolism, providing further evidence for the critical role of STPKs in regulating metabolism in *Streptomyces*.

Results

PknB is non-essential but regulates the timing of both development and antibiotic production

pknB was disrupted using transposon Tn*5062*. The insertion selected was located 372 base pairs from the ATG start codon, disrupting function of the kinase domain located between amino acid residues 11 and 277. Several independent mutants were easily obtained and verified by Southern hybridization. Although the *pknB* mutants grew similarly to the wild-type on MS medium, marked differences were observed between the parental and mutant strains grown on certain other media. For example, on 2xYT medium the mutants produced the blue pigmented actinorhodin earlier and in excess of the parental M145 strain (Fig. 1A) and on NE media, precocious aerial development and increased diffusible pigment synthesis were apparent for the mutants. Confirmation of the association of these phenotypic differences with disruption of *pknB* was obtained by genetic complementation, essentially restoring the wild-type phenotype to the complemented mutant strains (Fig. 1B).

Increased production of actinorhodin by the *pknB* mutant was quantified during growth in submerged culture. The mutant produced approximately four times the yield of the parental strain (Fig. 2), but the overall growth rate was unaffected. We have previously observed that addition of osmolyte stimulates production of actinorhodin by the parental strain M145 (Bishop *et al*., 2004).

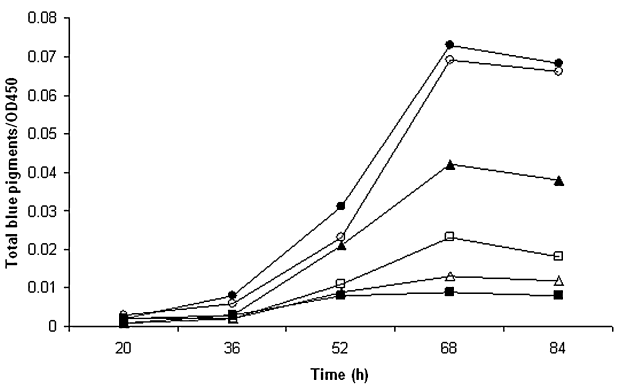

Fig. 2. Increased actinorhodin production by *pknB* and *fhaAB* mutants. The yields of actinorhodin and γ-actinorhodin at indicated time points relative to cell density (OD_{450}) were plotted for cultures grown in liquid R5 with or without addition of 250 mM NaCl. The values are averages of three independent experiments and standard deviations were <5% of the plotted values. (■/□) M145/ + NaCl; (▲/△) *pknB*/ + NaCl; (●/○) *fhaAB*/ + NaCl.

However, in contrast, actinorhodin production by the *pknB* mutant was partly suppressed by addition of osmolyte (Fig. 2).

Properties of PknB

PknB is predicted to be a 673-amino-acid membrane protein with the ability to autophosphorylate. To investigate these properties, recombinant N-terminal His-tagged PknB was expressed in *E. coli* BL21. After fractionation and Western blotting with an antibody to detect the His-tagged protein, PknB was predominantly found to be enriched in membrane fractions from *E. coli* (Fig. 3), migrating with an apparent approximate molecular mass of 130 kDa.

Recombinant His-tagged PknB was purified by ion-affinity chromatography. SDS-PAGE followed by Coomassie staining of column fractions revealed a single species of approximately 130 kDa (Fig. 4A). As the predicted size of PknB is 72 kDa, the identity of the purified protein with an apparent larger size was confirmed by extracting it from a gel, subjecting it to a tryptic digest, followed by liquid chromatography (LC) tandem mass spectrometry. All peptides from the digest matched those from an *in silico* digest of PknB. Anomalous migration in SDS-PAGE gels of STPKs and in particular PknB orthologues has been noted previously (Av-Gay *et al*., 1999; Fiuza *et al*., 2008). To examine phosphorylation of the recombinant kinase, we employed a phosphoprotein stain (Pro-Q Diamond) allowing for in-gel detection of phosphate groups attached to tyrosine, serine or threonine residues. Recombinant PknB was stained, indicating possible autophosphorylation in *E. coli* (Fig. 4B).

To investigate if phosphorylation in non-native *E. coli* was independent of ligand binding to the extracellular PASTA domains, a recombinant His-tagged protein

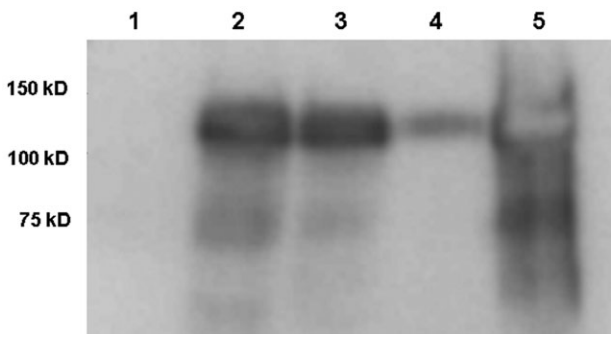

Fig. 3. Detection of PknB in cellular fractions of *E. coli*. PknB was detected with HRP conjugated anti penta – His antibody. Lane 1 = whole-cell extract (WCE) from uninduced *E. coli* transformed with pLK1. Lane 2 = WCE from induced cells containing pLK1. Lane 3 = insoluble fraction collected after centrifugation of WCE. Lane 4 = soluble fraction. Lane 5 = membrane fraction. Equal amounts of total protein were added to each lane.

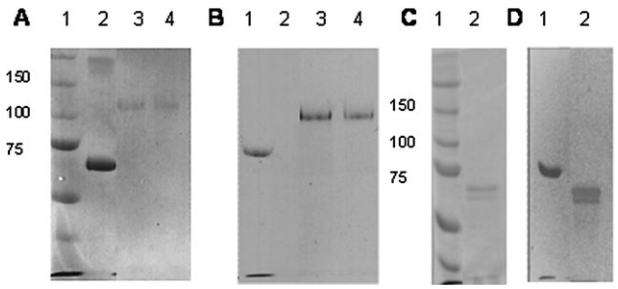

Fig. 4. Autophosphorylation of recombinant PknB. (A) and (C) are Coomassie-stained gels and (B) and (D) are the same gels, respectively, stained with Pro-Q Diamond stain. (A and B) Lane 1 = molecular weight markers; lane 2 = BSA; lanes 3 and 4 = purified recombinant PknB. (C and D) Lane 1 = molecular weight markers; lane 2 = purified cytoplasmic PknB kinase domain. Numbers to the left of (A) and (C) indicate the sizes (kDa) of molecular size markers (the 75 kDa protein is stained by Pro-Q Diamond).

containing just the cytoplasmic kinase domain was expressed. A soluble protein with an apparent mass of approximately 70 kDa (the expected mass was 36 kDa) was purified, together with a slightly smaller probable C-terminal truncated protein (Fig. 4C). The identity of the predominant larger protein as the N-terminal kinase domain of PknB was confirmed after LC tandem mass spectrometry of a tryptic digest (data not shown). Detection of this protein with the phosphoprotein stain indicated phosphorylation of the kinase domain (Fig. 4D).

Characterization of linked forkhead-associated protein genes

The conserved actinobacterial *pknB* gene cluster contains two neighbouring genes, *SCO3843* and *3844*, encoding forkhead-associated (FHA) proteins, hereafter termed *fhaA* and *fhaB*. It is emerging that FHA proteins are typical targets for phosphorylation by actinobacterial Ser/Thr kinases with, for example, mycobacterial PknB phosphorylating an orthologue of FhaA (Grundner *et al*., 2005). FHA proteins are believed to function as mediators of Ser/Thr kinase signalling. Thus, we investigated the consequences of loss of function of both *fhaA* and *fhaB* by constructing a double mutant, replacing the majority of the coding sequences for both genes by a hygromycin resistance gene. As with the *pknB* mutant, the *fhaAB* double mutant resembled the parental strain when grown on MS medium but exhibited precocious sporulation and antibiotic production on NE medium (Fig. 5A). Genetic complementation of the mutant with plasmid pSEF2, containing the *fhaAB* genes, restored the parental phenotype to the mutant (Fig. 5A). The yield of actinorhodin was quantified during growth in submerged culture, revealing that the *fhaAB* mutant produced approximately double the yield of the *pknB* mutant and

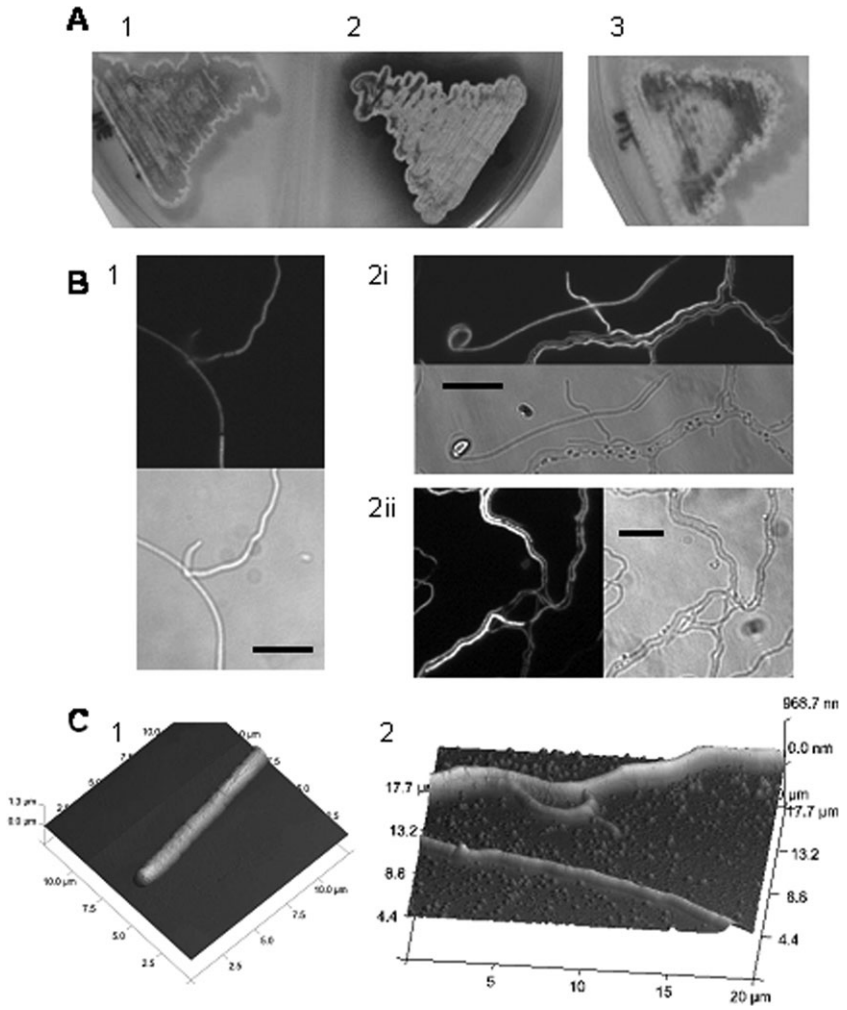

Fig. 5. Pleiotropic effects of disruption of *fhaAB* on growth and antibiotic production.
A. The parental M145 (1), the *fhaAB* mutant (2) and the complemented mutant (3) containing plasmid pSEF2 grown on NE medium for 72 h.
B. (1) Substrate hyphae of M145 visualized after staining with fluoroscein-conjugated wheat germ agglutinin (top), and the same field visualized by phase contrast microscopy; (2i top and bottom; 2ii left and right) similar images of the *fhaAB* mutant. Scale bars represent 10 μm.
C. AFM three-dimensional images derived from 'height' topographic measurements of (1) a substrate hypha of M145, and (2) a typical cord and a separate single hypha of the *fhaA* mutant. Note the partially emergent single hypha extruded from the cord.

eight times the yield of the parental strain (Fig. 2), but that growth rate was unaffected. The mutants also differed in that addition of osmolyte had no significant effect on the yields of the *fhaAB* mutant. As the function of the *pknB* gene cluster in other actinobacteria is primarily associated with growth and morphology, the observed accelerated differentiation of the mutants was further explored by examining cell morphologies. No gross differences could be detected between the substrate and aerial hyphae or spore chains of the parental strain M145 and the *pknB* mutant. In contrast, a large proportion of the substrate hyphae of the *fhaAB* mutant assembled as cords of between two and four hyphae growing together (Fig. 5B). There was no evidence of hyphal fusion as the hyphae growing in cords retained their individual cell walls, stained by fluoroscein-conjugated wheat germ agglutinin. These cords were not observed in the complemented *fhaAB* strain containing plasmid pSEF2. Staining with fluorescence-labelled vancomycin revealed no differences in the frequency of hyphal cross-walls between the mutant and wild-type (results not shown). We then examined the substrate hyphal cords of the mutant using atomic force microscopy. The topographic images obtained revealed up to 1 μm wide hyphae in the parental strain. In contrast, many hyphae of the *fhaAB* mutant were between 2 and 3 μm thick, consistent with cords comprised of multiple parallel hyphae longitudinally joined together (Fig. 5C). Apart from the dimensions, no differences could be detected between the surface of individual hyphae and that of the cords. The spore-bearing aerial hyphae of the *fhaAB* mutant did not assemble as cords and the surfaces of these hyphae and resulting spore chains appeared similar to those of the parental strain when examined using AFM, decorated with characteristic chaplin and rodlin assemblies (results not shown).

A snapshot comparison of phosphoproteomes

To gain insight into possible direct or indirect targets of PknB phsophorylation and FhaAB regulation, the phosphoproteomes of the parental strain M145 and the

mutants were compared by selective enrichment of Ser/Thr/Tyr phosphorylated proteins from whole-cell extracts. This preliminary study, identifying relatively abundant possible phosphorylated proteins enriched from the strains grown in one condition at a single time-point (NE medium, 48 h incubation), was designed simply to guide additional experimentation, rather than provide a systematic analysis of the different phosphoproteomes. Of 17 possible PknB targets not detected in the *pknB* mutant (Table 1), 6 were enzymes and 3 were proteins involved in transcription (RpoB) or protein biosynthesis (translation initiation factor and a chaperone). Of this latter category, all three have been identified as phosphorylated in other bacteria although the functional effects of post-translational modification are unknown. One possible phosphorylated enzyme, MurA, is involved in peptidoglycan biosynthesis, although it has not been previously identified as being phosphorylated in other bacteria.

Table 1. Putative phosphoproteins identified in either *S. coelicolor* M145 or the *fhaAB* mutant, but not in the *pknB* mutant.

SCO No.	Gene	Protein function	db[a]
(1) Putative phosphoproteins detected only in M145			
1296	–	Conserved hypothetical protein	–
1626	*rarE*	Putative cytochrome P450	+
1648	*arc*	AAA ATPase	–
2447	–	Hypothetical protein	–
2494	–	Putative pyruvate phosphate dikinase	–
2599	–	Hypothetical protein	–
2776	*accD1*	Acetyl/propionyl CoA carboxylase, beta subunit	–
3122	–	Probable nucleotidyltransferase	–
5199	–	Conserved hypothetical protein	–
5249	–	Putative nucleotide-binding protein	–
5373	*atpD*	ATP synthase beta chain	–
7516	*htpG*	heat shock protein	+
(2) Putative phosphoproteins detected in both M145 and the *fhaAB* mutant			
1662	–	Conserved hypothetical protein	–
2113	*bfr*	Probable bacterioferritin	+
2949	*murA*	UDP-*N*-acetylglucosamine transferase	–
4654	*rpoB*	DNA-directed RNA polymerase beta chain	+
5706	–	Probable translational initiation factor	+
(3) Putative phosphoproteins detected only in the *fhaAB* mutant			
0985	*metE*	Putative methionine synthase	–
1476	*metK*	S-adenosylmethionine synthetase	+
1968	–	Putative secreted glycerophosphoryl diester phosphodiesterase	–
2620	–	Putative cell division trigger factor	+
2736	*citA*	Citrate synthase	+
3122	–	Putative nucleotidyltransferase	–
3127	*ppc*	Phosphoenolpyruvate carboxylase	+
3928	*thiC*	Probable thiamine biosynthesis protein	–
5281	–	Probable 2-oxoglutarate dehydrogenase	+
5838	–	Putative protease	–
6198	–	Putative secreted protein	–
6199	–	Secreted esterase	–

a. A plus indicates that an orthologous protein is found in the (Bacterial) Phosphorylation Site Database (http://www.phosphorylation.biochem.vt.edu/xpd.htm).

An overwhelming majority (10/12) of phosphorylated proteins detected only in the *fhaAB* mutant were enzymes (Table 1). Of these, six are involved in primary metabolism. Of note in relation to the interplay between primary and secondary metabolisms are two enzymes involved in synthesis of S-adenosylmethionine [methionine synthase and S-adenosylmethionine (SAM) synthetase] and three enzymes involved in central carbon metabolism (citrate synthase, 2-oxoglutarate dehydrogenase and phosphoenolpyruvate carboxylase). Four of these five enzymes have been identified as being phosphorylated in other bacteria, but functional attributes of the modifications have not been determined.

The fhaAB *mutant has a deregulated TCA cycle favouring antibiotic production*

Wild-type *S. coelicolor* grown on a glucose carbon source initially acidifies its immediate environment due to secretion of organic acid TCA cycle intermediates. As the developmental cycle proceeds, these organic acids are metabolized and consequently the surrounding pH increases to neutral. Aconitase and citrate synthase mutants affected in key steps in the TCA cycle are prone to irreversible medium acidification, reflecting overall reduced TCA cycle activity (Viollier *et al*., 2001a,b). To assess possible deregulation of the TCA cycle due to enzyme phosphorylation, medium acidification by the *fhaAB* mutant was examined by inclusion of a pH indicator in the growth medium (Fig. 6A). Phenol red indicator changes colour from yellow to red as pH increases from 6.6 to 8.0, allowing real-time visual analysis of any pH changes. After 48 h growth of the wild-type, any secreted organic acids were consumed, reversing initial acidification of the medium that occurs even with inclusion of 10 mM MES buffer. In contrast, although further advanced in the developmental cycle as evidenced by some sparse aerial growth and precocious antibiotic production, after 48 h growth the growth medium surrounding the *fhaAB* mutant remained acidic with only partial reversal in a 2–3 mm border surrounding the culture. This retarded reversal continued over extended incubations. Similar analysis of the *pknB* mutant revealed no significant difference in acidogenesis between it and the wild-type (results not shown).

These observations were consistent with reduced TCA cycle activity during the first 48 h of growth, but with an increased flux of precursors, for example acetyl CoA, channelled to antibiotic biosynthesis by the *fhaAB* mutant. To attempt to identify key metabolic nodes affecting TCA cycle activity and antibiotic production, both the wild-type and *fhaAB* mutant were grown on mannitol soy medium lacking glucose but supplemented with various metabolic intermediates. The non-supplemented growth medium

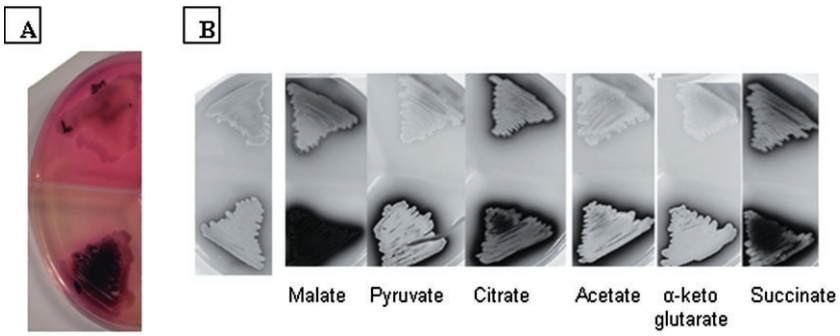

Fig. 6. Acidogenesis and stimulation of antibiotic production by intermediates of central carbon metabolism.
A. M145 (top) and the *fhaAB* mutant (bottom) were grown for 48 h on NE medium initially buffered to pH 7.1 with 10 mM MES buffer and with inclusion of phenol red as pH indicator.
B. M145 (top) and the *fhaAB* mutant were grown for 72 h on MS medium (left) or MS medium containing different TCA cycle intermediates [10 mM] as indicated.

does not support antibiotic production by the wild-type, although the *fhaAB* mutant produced a little (Fig. 6B). However, inclusion of 10 mM malate, citrate or succinate stimulated some production by the wild-type and even more by the mutant. Of these intermediates, addition of malate and, to some extent, succinate exacerbated the inability of the mutant to reverse acidogenesis to the extent that aerial development was inhibited. Notably, inclusion of either pyruvate or acetate had no effect on the lack of antibiotic biosynthesis by wild-type, but had a marked positive stimulus on the yields of the mutant.

Discussion

With respect to some aspects of structure and function, PknB of *S. coelicolor* appears to be similar to the better characterized orthologue PknB of *M. tuberculosis* (Av-Gay *et al*., 1999; Boitel *et al*., 2003; Fernandez *et al*., 2006). They share a common domain architecture with 41% overall identity of amino acid sequence. This study indicates that recombinant *S. coelicolor* PknB is a membrane protein, as predicted, and that the recombinant full-length protein is phosphorylated in *E. coli*, as previously indicated to be the case for *M. tuberculosis* PknB (Av-Gay *et al*., 1999). STPKs exist constitutively in a non-phosphorylated 'off' state, and are activated by, for example, ligand binding. Indeed, based on structural studies, it is suggested that inactive non-phosphorylated PknB monomers dimerize by virtue of ligand binding (Mieczkowski *et al*., 2008; Barthe *et al*., 2010). The dimer adopts a conformation that is activated for both autophosphorylation and substrate phosphorylation. For actinomycete PknBs the ligand(s) are suspected to be peptidoglycan stem peptides that are recognized by extracellular PASTA domains (Yeats *et al*., 2002; Jones and Dyson, 2006). Indeed in the firmicute *Bacillus subtilis*, peptidoglycan fragments that specifically contain m-Dpm (meso-diaminopimelic acid), and not L-Lys, at the third position of the stem peptide activate a PrkC (PknB orthologue)-dependent signalling pathway (Shah *et al*., 2008). *S. coelicolor* stem peptides contain L,L-Dpm at the third position and can substitute for m-Dpm stem peptides to activate *B. subtilis* PrkC. So it is possible that m-Dpm containing stem peptides produced by *E. coli* can activate recombinant *S. coelicolor* PknB. However, efficient phosphorylation of the truncated N-terminal cytoplasmic kinase domain of *S. coelicolor* PknB expressed in *E. coli* suggests ligand-independent phosphorylation. Purified recombinant forms of both the full-length and the cytoplasmic catalytic domain of *M. tuberculosis* PknB can autophosphorylate *in vitro* (Av-Gay *et al*., 1999; Boitel *et al*., 2003), suggesting that ligand binding either may not be a requisite for PknB activation or that the *in vitro* conditions in some way facilitate ligand-independent activation. Another scenario is that activation of non-phosphorylated PknB or signal transduction by the autophosphorylated kinase is modulated *in vivo* by binding of an additional factor to the catalytic domain.

PrkC in *B. subtilis* is required to trigger spore germination in response to peptidoglycan fragments (Shah *et al*., 2008). In actinomycetes, *pknB* is part of a conserved gene cluster, termed the *pknB* cluster (Molle and Kremer, 2010), encoding both morphogenetic and signalling proteins. In *M. tuberculosis*, *pknB* is an essential gene and manipulation of its expression alters cell shape (Kang *et al*., 2005); current knowledge on its role in regulation of cell shape and cell division has been recently reviewed (Molle and Kremer, 2010). Indeed, an *in vivo* target of PknB phosphorylation in *M. tuberculosis* is a penicillin binding protein, PBPA, involved in cell wall synthesis and encoded by a gene in the *pknB* cluster (Dasgupta *et al*., 2006). PknB can also phosphorylate PknA, a second STPK encoded by the immediate neighbouring gene in the cluster (Kang *et al*., 2005), which can in turn phosphorylate the critical cell division protein FtsZ (Thakur and Chakraborti, 2006). Moreover, PknB also phosphorylates Wag31, an orthologue of the morphogenetic DivIVA protein (Kang *et al*., 2005). In another actinomycete, *Corynebacterium glutamicum*, there is conflicting evidence as to whether *pknB* is essential (Fiuza *et al*., 2008; Schultz *et al*., 2009), but manipulation of its expression alters cell morphology and FtsZ has been identified as a phosphorylation substrate (Schultz *et al*., 2009). In *Streptomyces*, the *pknB* gene cluster is similar except that an

orthologue for *pknA* is absent. Our analysis indicates that *pknB* is non-essential and we could detect no changes in cell morphology at any stage of the developmental cycle in a *pknB* mutant. Instead, the phenotype of the mutant is consistent with a role for PknB in regulating timing of the developmental cycle, including antibiotic production. Increased antibiotic production could be related to an absence of detectable phosphorylated RpoB in the phosphoproteome of the *pknB* mutant; mutations in *rpoB* that increase antibiotic production are documented (Hu *et al*., 2002; Lai *et al*., 2002). Although it has been suggested that these mutations could mimic a conformational change brought about by binding of ppGpp, such a change could also be induced by protein phosphorylation. In addition, the observation that precocious production and overall yields of antibiotic biosynthesis by the mutant can be suppressed by osmolyte suggests the possibility of regulation of alternative sigma factor activity. For example, SigH is required for the osmotic stress response and is regulated by its anti-sigma factor PrsH (Viollier *et al*., 2003). A *prsH* mutant, with increased SigH activity, overproduces antibiotic. In response to salt stress, PknB could phosphorylate PrsH, thereby activating SigH. A precedent for this type of regulation is phosphorylation by PknB of the anti-sigma factor RshA in *M. tuberculosis* (Park *et al*., 2008). The low abundance of sigma and anti-sigma factors would militate against detection of phosphorylated forms in the snapshot phosphoproteome analysis we performed.

The FHA domains mediate protein–protein interactions through recognition of phosphorylated threonine residues and often act as mediators of protein–protein interactions in STPK signal transduction (Durocher and Jackson, 2002). Moreover, *in vivo* STPK-mediated phosphorylation of FHA-domain proteins themselves has been documented in *Actinobacteria* with, for example, GarA and OdhI being substrates for phosphorylation by PknB in *M. tuberculosis* and *C. glutamicum* respectively (Villarino *et al*., 2005; Schultz *et al*., 2009). For these examples, phosphorylation of the FHA-domain protein acts as a switch whereby it no longer binds and inhibits a target enzyme involved in glutamate metabolism in *M. tuberculosis* and the TCA cycle in *C. glutamicum* respectively (O'Hare *et al*., 2008; Barthe *et al*., 2009). The mycobacterial orthologues of *S. coelicolor* FhaA and FhaB are, respectively, Rv0019c and Rv0020c. At least *in vitro*, both of these latter proteins are substrates for PknB phosphorylation (Grundner *et al*., 2005; Gupta *et al*., 2009), although we failed to detect either in our snapshot phosphoproteome analysis, which may simply reflect their low abundance in the experimental conditions used. The *in vitro* evidence for phosphorylation of the mycobacterial proteins, and their conserved genetic association with *pknB*, suggests either or both FHA-domain proteins may be important mediators of PknB signal transduction, prompting investigation into the consequences of their loss of function in *S. coelicolor*. Similar to the *pknB* mutant, the *fhaAB* mutant exhibited accelerated development and antibiotic production. However, closer inspection revealed fundamental differences. The *fhaA* mutant has an obvious morphological phenotype in that two or three individual substrate hyphae have a tendency to aggregate together linearly and grow as a fused cord-like structure, somewhat reminiscent of fungal mycelial cords. We are not aware of previous reports of 'cording' in *Streptomyces*, although it is well-documented in non-hyphal mycobacteria where cell surface mycolic acids are believed to play a role in the formation of linear aggregates of cells (Glickman *et al*., 2000; Julian *et al*., 2010). In the absence of a mycolic acid layer, other cell wall components in the *fhaAB* mutant presumably promote hyphal aggregation. At the onset of aerial development the hyphal surface is normally modified by decoration with assemblies of amphipathic proteins, the chaplins (Claessen *et al*., 2003; Elliot *et al*., 2003; Del Sol *et al*., 2007). This modification to the surface of the aerial hyphae may account for the lack of any detectable cording of these hyphae of the *fhaAB* mutant.

The *pknB* and *fhaAB* mutants also differed with respect to their precocious antibiotic production. The latter overproduced actinorhodin to a greater extent and this was not suppressed by salt as in the case of the *pknB* mutant. Moreover, the propensity for the *fhaAB* mutant to acidify the surrounding media is evidence for deregulated TCA cycle activity. An inability to reverse medium acidification was originally described for citrate synthase and aconitase mutants which, in contrast to the *fhaAB* mutant, were impaired in antibiotic biosynthesis (Viollier *et al*., 2001a,b). The imbalance in metabolism in the *fhaAB* mutant, with precocious actinorhodin production, suggests that carbon flux is prematurely diverted away from the TCA cycle towards secondary metabolism, presumably via acetyl-CoA. Consistent with this hypothesis, feeding with C2 (acetate) or C3 (pyruvate) compounds specifically stimulated actinorhodin production by the *fhaAB* mutant, whereas C4+ TCA cycle intermediate compounds were non-specific in their effect. In addition, phosphoproteome analysis of the *fhaAB* mutant revealed phosphorylation of two TCA cycle enzymes, citrate synthase and 2-oxoglutarate dehydrogenase, and one anaplerotic enzyme, phosphoenolpyruvate carboxylase. Taken together, this indicates that phosphorylation of these enzymes could regulate their activity, effecting a switch from central carbon metabolism to secondary metabolism. The phosphoproteome analysis also provided another possible clue to explain the overproduction of actinorhodin with evidence for phosphorylation of SAM synthetase. Previous reports have indicated that

overexpression of this enzyme, resulting in increased intracellular SAM, stimulates actinorhodin production in *S. lividans*, a close relative of *S. coelicolor*, due to increased transcription of the pathway-specific regulatory gene *actII-ORF4* (Kim *et al*., 2003; Okamoto *et al*., 2003). Phosphorylation of SAM synthetase could potentially have a similar effect.

These data provide evidence that FhaAB play a key role in *Streptomyces*, presumably by modulating STPK signalling *in vivo*. There are five other predicted FHA-domain proteins encoded by *S. coelicolor*, with two of these genetically linked to other STPKs (Pallen *et al*., 2002). The genetic association suggests that FHA proteins are likely to regulate their cognate STPKs, as supported in the case of the FhaAB orthologues of *M. tuberculosis* that interact with PknB *in vitro* (Grundner *et al*., 2005; Gupta *et al*., 2009). However, just as there is evidence for promiscuous STPK substrate phosphorylation (Horinouchi, 2003; Chao *et al*., 2010), cross-regulation by a given FHA-domain protein of different STPKs is also possible (Grundner *et al*., 2005). We suspect that FhaAB inhibit phosphorylation by STPKs, including PknB, of target proteins by binding to the catalytic kinase domain. It is illuminating that *in vitro* the FhaA orthologue, Rv0019c, can bind to both non-phosphorylated and autophosphorylated PknB (Gupta *et al*., 2009). We are now investigating interactions of *S. coelicolor* FHA proteins with both their cognate and non-cognate STPKs. Removal of the 'brakes' to STPK-mediated phosphorylation, possibly by phosphorylation of FHA-domain proteins themselves, or experimentally by gene inactivation as we have demonstrated, can help to reveal the important role of STPKs in regulating bacterial physiology, in this case antibiotic production by *Streptomyces*.

Experimental procedures

Bacterial strains and media

Streptomyces coelicolor A3(2) and *Escherichia coli* strains are listed and described in Table 2. Cloning procedures were performed in *E. coli* JM109, while *E. coli* ET12567/pUZ8002

Table 2. Bacterial strains, plasmids and cosmids.

Strain or plasmid	Description	Source
Streptomyces		
S. coelicolor A3(2) M145	Prototrophic SCP1– SCP2– Pgl+	Kieser *et al*. (2000)
pknB	M145 *pknB*$^-$:Tn*5062* (4233963)	This study
fhaAB	M145 Δ*fhaAB*::Tn*5066*	This study
E. coli		
JM109	F' *traD36 proA*$^+$*B*$^+$ *lacIq* Δ*(lacZ)M15/*Δ*(lac–proAB) glnV44 e14– gyrA96 recA1 relA1endA1 thi hsdR17*	Yanisch-Perron *et al*. (1985)
E. coli ET12567 (pUZ8002)	*dam13*::Tn*9 dcm6 hsdM hsdR recF143* 16 z*jj201*::Tn*10 galK2 galT22 ara14 lacY1 xyl5 leuB6 thi1 tonA31 rpsL136 hisG4 tsx78 mtli glnV44*, containing the non-transmissible *oriT* mobilizing plasmid, pUZ8002	Flett *et al*. (1997)
BL21(DE3)pLysS	F$^-$ *ompT hsdS*$_B$ (r_B^- m_B^-) *gal dcm* (DE3) pLysS	Novagen
Cosmids		
SCH69	Supercos-1 with *S. coelicolor* DNA	Redenbach *et al*. (1996)
SCH69.2.F01	SCH69 with Tn*5062* insertion at position 23524	Bishop *et al*. (2004)
SCH69.1.E10	SCH69 with Tn*5062* insertion at position 26140	Bishop *et al*. (2004)
SCH69.2.B04	SCH69 with Tn*5062* insertion at position 16172	Bishop *et al*. (2004)
Plasmids		
pME6	*E. coli* cloning vector; kanamycin and ampicillin resistance	Fernandez Martinez *et al*. (2009)
pQM5066	pMOD+Tn*5066*; hygromycin and ampicillin resistance	Facey *et al*. (2009)
pALTER1	*E. coli* cloning vector; tetracycline resistance	Promega Corp.
pET16b	*E. coli* cloning vector; kanamycin resistance	Novagen
pSH152	Shuttle vector; hygromycin resistance	Mistry *et al*. (2008)
pSET152	Shuttle vector; apramycin resistance	Bierman *et al*. (1992)
pUWL219	Shuttle vector; ampicillin and thiostrepton resistance	Wehmeier (1995)
pLK2	pALTER1 containing *pknB*	This study
pSC3848	pSH152 containing *pknB*	This study
pHit-K	pLK2 with NdeI site	This study
pHit-K2	pHitK with additional NdeI site	This study
pETK1	pET16b with *pknB*	This study
pETK2	pET16b with *pknB* kinase domain	This study
pMER	pME6 with *fhaAB* right-hand flanking sequence	This study
pMERL	pMER with *fhaAB* left-hand flanking sequence	This study
pMERL66	pMERL with Tn*5066*	This study
pRCLU2	pUWL219 with SphI fragment from SCH69.2.B04	This study
pSEF2	pSET152 with *fhaAB*	This study

was used for intergeneric conjugative transfer of plasmid DNA into *Streptomyces* strains (Kieser *et al*., 2000). *E. coli* BL21 was used to express recombinant forms of PknB. Culturing of *E. coli* strains was as recommended (Sambrook and Russell, 2001). *Streptomyces coelicolor* strains were grown on the following solid media, supplemented as indicated: MS (mannitol soya flour) agar, NE agar, 2xYT agar or in submerged culture in liquid R5 medium (Kieser *et al*., 2000). *Streptomyces* mutant strains were obtained using a Tn*5062* mutagenized cosmid or plasmid pMERL66 (Table 2) after conjugation from *E. coli* (Bishop *et al*., 2004). The nature of the mutations was confirmed by Southern blot (Sambrook and Russell, 2001).

DNA manipulation and plasmid construction

Standard DNA procedures were performed as described (Sambrook and Russell, 2001). To construct a *pknB* complementing plasmid, a 5.95 kb KpnI fragment containing *pknB* was released from cosmid SCH69.1.E10 and ligated into pAlter1 (also cut with KpnI) to form pLK2. This plasmid was then cut with restriction enzymes BamHI and EcoICRI to release a 3.8 kb fragment that was blunt – ended using SI nuclease. This fragment, containing *pknB* and 748 bp of upstream sequence was then ligated into pSH152 cut with EcoRV to create plasmid pSC3848. To overexpress PknB in *E. coli*, an NdeI site overlapping the ATG start codon of the gene in pLK2 was introduced by site-directed mutagenesis (QuikChangeXL, Stratagene) using oligonucleotides PknNdef (5′-GGCTGGTAGGTACATATGGAAGAGCCG) and PknNder (5′-CGGCTCTTCCATATGTACCTACCAGCC), resulting in plasmid pHit-K. An NdeI–BamHI fragment was then subcloned into pET16b, generating the plasmid pETK1 for expression of PknB with an N-terminal deca-histidine tag. To overexpress just the kinase domain, primers MidKin1 (5′-CGATCTTCCTGCATATGGCGGGCGTCC) and MidKin2 (5′-GGACGCCCGCCATATGCAGGAAGATCG) were used in a site-directed mutagenesis reaction with pHit-K to introduce an NdeI site in the middle of the transmembrane domain, resulting in plasmid pHit-K2. A 1060 bp NdeI fragment was released from pHit-K2 and ligated into pET16b to form plasmid pETK2. To inactivate *fhaAB* required enough DNA either side of internally deleted copies of the two genes. To do this, relevant fragments were cloned from cosmid H69 into the multiple cloning site of plasmid pME6 as follows: the 'right hand' 3756 bp NotI–XhoI fragment was ligated into pME6, yielding the intermediate plasmid pMER, followed by addition of the 3065 bp 'left hand' BglII fragment at the BamHI site, creating plasmid pMERL. This plasmid contains 632 bp of the beginning of *fhaA* (the FHA domain is encoded by the region extending from 648 to 795 bp) and the last 306 bp of *fhaB* but with >2 kb of flanking sequences on either side. Subsequently, a copy of Tn*5066* as a PvuII fragment was inserted at an EcoRV site at the junction of the right and left hand fragments, creating pMERL66. The transposon provided a convenient way of introducing both an origin of transfer and a selectable antibiotic resistance marker (in this case, hygromycin). An *fhaAB* complementing plasmid was derived by first cloning a 10.3 kb SphI fragment spanning *fhaA* to *SCO3847* into pUWL219, resulting in pRCLU2. From this a 2.68 kb PvuII–EcoRV fragment containing *fhaAB* was subcloned into pSET152, creating pSEF2.

Protein methods

To purify recombinant forms of PknB, 1 ml of a fresh stationary phase culture of *E. coli* BL21 cells containing the appropriate plasmid was inoculated into 24 ml Luria–Bertani plus kanamycin and grown at 37°C, 225 r.p.m. in a shake flask for 4–6 h. To induce overexpression, IPTG was added to the culture to a final concentration of 10 mM and shaken at 30°C, 225 r.p.m. for 1–3 h. Following induction, the cells were pelleted and resuspended in 5 ml sonication buffer [50 mM Tris-HCl, pH 8, 200 mM NaCl, 15 mM EDTA, with complete protease inhibitor cocktail (Roche Diagnostics)] prior to sonication to disrupt the cells and provide a whole-cell extract. This was spun in a centrifuge at 15 000 *g* for 5 min to remove intact cells and inclusion bodies, with the pellet providing the insoluble fraction. The supernatant (containing membrane and soluble fractions) was then taken and centrifuged at 100 000 *g* for 1 h in an ultracentrifuge. The supernatant (soluble fraction) was then decanted and kept, while the pelleted membrane fraction was suspended in sonication buffer containing 2% w/v Triton X-100. To maximize recovery in subsequent PknB purification, 8 M urea was employed to denature any insoluble PknB and 2% w/v Triton X-100 was used to disrupt membranes. For metal-affinity chromatography, a His-Trap system (GE Healthcare) was employed following the manufacturer's recommendations, using 10 and 300 mM imidazole buffers, respectively, for column washing and protein elution. Total protein concentration was determined using the Bradford method (Bio-Rad). SDS-PAGE was performed as previously described (Sambrook and Russell, 2001), loading 10 μg total protein per lane in 15% SDS-PAGE gels. Proteins were transferred to a polyvinylidene difluoride (PVDF) membrane (Hybond-P, Amersham) using a semi-dry electrophoretic transfer cell (Trans-Blot SD, Bio-Rad). Immunological detection was performed using an ECL Advance Western blotting detection kit (Amersham Pharmacia Biotech). His-tagged proteins were detected with a Penta-His peroxidase conjugate (Qiagen). To investigate PknB phosphorylation, gels were stained with Pro-Q Diamond stain (Invitrogen) as per the manufacturer's instructions.

For analysis of the phosphoproteomes of *Streptomyces* strains, sterile cellophane discs placed on top of NE plates were inoculated with *Streptomyces* spores, and incubated for 48 h at 30°C. Mycelia were scraped from the cellophane discs and suspended in sonication buffer. Cells were disrupted by sonication (20-sec burst on ice) until a clear lysate was obtained. Cell-free extracts were obtained by centrifugation (15 000 *g* for 3 min) and recovery of the supernatant. To enrich for phosphoproteins, affinity chromatography was employed using a Phosphoprotein purification kit (Qiagen) as per the manufacturer's instructions. Retained and subsequently eluted proteins were concentrated using Nanosep columns supplied with the kit. Enrichment was monitored by SDS-PAGE of cell-free extracts and column fractions followed by detection of phosphoproteins with Pro-Q Diamond stain (Fig. S1). For mass-spectrometry based identification of proteins, fractions enriched in phosphoproteins were separated by SDS-PAGE and stained with Coomassie blue. Gel

slices (20 per lane) spanning the range of detectable proteins were excised and transferred to microfuge tubes. The pH was corrected with a brief wash in 100 mM NH_4HCO_3. The gel pieces were then destained with the addition of 200 μl 50% acetonitrile/50% 50 mM NH_4HCO_3 and vortexed, followed by 10 min incubation at room temperature. This step was repeated until all stain had been washed from the gel pieces. Excess liquid was removed, and the pieces were washed for 5 min in 200 μl 50% acetonitrile/50% 50 mM NH_4HCO_3. The gel pieces were dehydrated with 100% acetonitrile, followed by drying in a rotary evaporator. The gel pieces were then rehydrated in buffer containing 50 mM NH_4HCO_3 and trypsin (20 ng μl^{-1}). The digest was then incubated overnight at 37°C. Any supernatant present was transferred to a clean microfuge tube, and 30 μl 50% acetonitrile/2% formic acid was added to the gel pieces. After a 20 min incubation with vortexing, the pieces were sonicated briefly, then spun and the supernatant was added to the original supernatant. This step was repeated to give a final volume of around 60 μl. This volume was vortexed and then reduced in volume to 5–10 μl. After a final 10 min centrifugation at 15 000 *g*, the sample was ready for loading. HPLC-MS/MS was carried out using a nano-ESI ion trap, the LCQ DECA XP (ThermoFinnigan, Hemel Hempstead, UK), equipped with a nanospray interface. For the HPLC separation of the peptide sample, a 10 μl sample was injected using a FAMOS autosampler (Dionex) onto an in-house prepared fused silica C_{18} PepMap column (15 cm × 75 μm) with a pulled tip that formed the electrospray needle thereby eliminating any dead volume after the column. The sample was injected into a mobile phase of 2% acetonitrile, 98% water (0.1% formic acid) (mobile phase A) with mobile phase B representing 0.1% formic acid in acetonitrile. After loading the sample for 5 min, a gradient between 100% A and 60% B over 45 min was performed followed by an increase to 96% B over 15 min, washing of the column with 95% B for 10 min before returning to 100% A mobile phase composition, and column re-equilibration over 10 and 15 min respectively. The mobile phase was delivered by an Ultimate pump system with a nanoflow cartridge split system (Dionex). A spray voltage of 1.6 kV was applied to the sample at a liquid junction just prior to the column, and the spray passed into a heated capillary at 165°C and a capillary voltage of 10 V. Data were acquired in a positive, data-dependent acquisition mode in which the mass spectrometer first acquires a full scan mass spectrum between 475 and 2000 Da. The MS/MS spectra of the three most abundant ions in the spectrum were then obtained before another full scan spectrum was again monitored. This process was repeated throughout the HPLC-MS/MS run with dynamic exclusion parameters excluding any ions whose MS/MS spectra were obtained three times from further analysis for 3 min. The proteins in gel slices were identified from selected peptide spectra obtained by nano-ESI-ion trap MS/MS using Bioworks Browser version 3.2 (ThermoElectron), which compared the spectra produced against a non-redundant database of all organisms.

Microscopy

Strains used for fluorescence microscopy were grown in the acute angle of a coverslip inserted in NE agar medium. Staining of live cell walls was done using fluoroscein-conjugated wheat germ agglutinin (Invitrogen) as previously described (Del Sol *et al*., 2007). Images were obtained using a Nikon Eclipse E600 epifluorescence microscope fitted with a Coolsnap microscope camera (RS Photometrics., Tucson, AZ, USA). Atomic Force Microscopy (AFM) samples were prepared and imaged as described previously (Del Sol *et al*., 2007).

Acknowledgements

G.J. was supported by a BBSRC studentship. P.D. acknowledges support from the CEC (FP6 LSH IP 005224) and BBSRC (BB/E019242/1).

References

Av-Gay, Y., Jamil, S., and Drews, S.J. (1999) Expression and characterization of the *Mycobacterium tuberculosis* serine/threonine protein kinase PknB. *Infect Immun* **67:** 5676–5682.

Barthe, P., Roumestand, C., Canova, M.J., Kremer, L., Hurard, C., Molle, V., and Cohen-Gonsaud, M. (2009) Dynamic and structural characterization of a bacterial FHA protein reveals a new autoinhibition mechanism. *Structure* **17:** 568–578.

Barthe, P., Mukamolova, G.V., Roumestand, C., and Cohen-Gonsaud, M. (2010) The structure of PknB extracellular PASTA domain from *mycobacterium tuberculosis* suggests a ligand-dependent kinase activation. *Structure* **18:** 606–615.

Bentley, S.D., Chater, K.F., Cerdeno-Tarraga, A.M., Challis, G.L., Thomson, N.R., James, K.D., *et al*. (2002) Complete genome sequence of the model actinomycete *Streptomyces coelicolor* A3(2). *Nature* **417:** 141–147.

Bibb, M. (1996) 1995 Colworth Prize Lecture. The regulation of antibiotic production in *Streptomyces coelicolor* A3(2). *Microbiology* **142:** 1335–1344.

Bierman, M., Logan, R., O'Brien, K., Seno, E.T., Rao, R.N., and Schoner, B.E. (1992) Plasmid cloning vectors for the conjugal transfer of DNA from *Escherichia coli* to *Streptomyces* spp. *Gene* **116:** 43–49.

Bishop, A., Fielding, S., Dyson, P., and Herron, P. (2004) Systematic insertional mutagenesis of a streptomycete genome: a link between osmoadaptation and antibiotic production. *Genome Res* **14:** 893–900.

Boitel, B., Ortiz-Lombardia, M., Duran, R., Pompeo, F., Cole, S.T., Cervenansky, C., and Alzari, P.M. (2003) PknB kinase activity is regulated by phosphorylation in two Thr residues and dephosphorylation by PstP, the cognate phospho-Ser/Thr phosphatase, in *Mycobacterium tuberculosis*. *Mol Microbiol* **49:** 1493–1508.

Chao, J., Wong, D., Zheng, X., Poirier, V., Bach, H., Hmama, Z., and Av-Gay, Y. (2010) Protein kinase and phosphatase signaling in *Mycobacterium tuberculosis* physiology and pathogenesis. *Biochim Biophys Acta* **1804:** 620–627.

Chater, K.F. (2001) Regulation of sporulation in *Streptomyces coelicolor* A3(2): a checkpoint multiplex? *Curr Opin Microbiol* **4:** 667–673.

Claessen, D., Rink, R., de Jong, W., Siebring, J., de Vreugd, P., Boersma, F.G., *et al*. (2003) A novel class of secreted

hydrophobic proteins is involved in aerial hyphae formation in *Streptomyces coelicolor* by forming amyloid-like fibrils. *Genes Dev* **17:** 1714–1726.

Cole, S.T., Brosch, R., Parkhill, J., Garnier, T., Churcher, C., Harris, D., *et al*. (1998) Deciphering the biology of *Mycobacterium tuberculosis* from the complete genome sequence. *Nature* **393:** 537–544.

Dasgupta, A., Datta, P., Kundu, M., and Basu, J. (2006) The serine/threonine kinase PknB of *Mycobacterium tuberculosis* phosphorylates PBPA, a penicillin-binding protein required for cell division. *Microbiology* **152:** 493–504.

Del Sol, R., Armstrong, I., Wright, C., and Dyson, P. (2007) Characterization of changes to the cell surface during the life cycle of *Streptomyces coelicolor*: atomic force microscopy of living cells. *J Bacteriol* **189:** 2219–2225.

Durocher, D., and Jackson, S.P. (2002) The FHA domain. *FEBS Lett* **513:** 58–66.

Elliot, M.A., Karoonuthaisiri, N., Huang, J., Bibb, M.J., Cohen, S.N., Kao, C.M., and Buttner, M.J. (2003) The chaplins: a family of hydrophobic cell-surface proteins involved in aerial mycelium formation in *Streptomyces coelicolor*. *Genes Dev* **17:** 1727–1740.

Facey, P.D., Hitchings, M.D., Saavedra-Garcia, P., Fernandez-Martinez, L., Dyson, P.J., and Del Sol, R. (2009) *Streptomyces coelicolor* Dps-like proteins: differential dual roles in response to stress during vegetative growth and in nucleoid condensation during reproductive cell division. *Mol Microbiol* **73:** 1186–1202.

Fernandez Martinez, L., Bishop, A., Parkes, L., Del Sol, R., Salerno, P., Sevcikova, B., *et al*. (2009) Osmoregulation in *Streptomyces coelicolor*: modulation of SigB activity by OsaC. *Mol Microbiol* **71:** 1250–1262.

Fernandez, P., Saint-Joanis, B., Barilone, N., Jackson, M., Gicquel, B., Cole, S.T., and Alzari, P.M. (2006) The Ser/Thr protein kinase PknB is essential for sustaining mycobacterial growth. *J Bacteriol* **188:** 7778–7784.

Fiuza, M., Canova, M.J., Zanella-Cleon, I., Becchi, M., Cozzone, A.J., Mateos, L.M., *et al*. (2008) From the characterization of the four serine/threonine protein kinases (PknA/B/G/L) of *Corynebacterium glutamicum* toward the role of PknA and PknB in cell division. *J Biol Chem* **283:** 18099–18112.

Flett, F., Mersinias, V., and Smith, C.P. (1997) High efficiency intergeneric conjugal transfer of plasmid DNA from *Escherichia coli* to methyl DNA-restricting streptomycetes. *FEMS Microbiol Lett* **155:** 223–229.

Glickman, M.S., Cox, J.S., and Jacobs, W.R., Jr (2000) A novel mycolic acid cyclopropane synthetase is required for cording, persistence, and virulence of *Mycobacterium tuberculosis*. *Mol Cell* **5:** 717–727.

Grundner, C., Gay, L.M., and Alber, T. (2005) *Mycobacterium tuberculosis* serine/threonine kinases PknB, PknD, PknE, and PknF phosphorylate multiple FHA domains. *Protein Sci* **14:** 1918–1921.

Gupta, M., Sajid, A., Arora, G., Tandon, V., and Singh, Y. (2009) Forkhead-associated domain-containing protein Rv0019c and polyketide-associated protein PapA5, from substrates of serine/threonine protein kinase PknB to interacting proteins of *Mycobacterium tuberculosis*. *J Biol Chem* **284:** 34723–34734.

Hesketh, A., Bucca, G., Laing, E., Flett, F., Hotchkiss, G., Smith, C.P., and Chater, K.F. (2007a) New pleiotropic effects of eliminating a rare tRNA from *Streptomyces coelicolor*, revealed by combined proteomic and transcriptomic analysis of liquid cultures. *BMC Genomics* **8:** 261.

Hesketh, A., Chen, W.J., Ryding, J., Chang, S., and Bibb, M. (2007b) The global role of ppGpp synthesis in morphological differentiation and antibiotic production in *Streptomyces coelicolor* A3(2). *Genome Biol* **8:** R161.

Horinouchi, S. (2003) AfsR as an integrator of signals that are sensed by multiple serine/threonine kinases in *Streptomyces coelicolor* A3(2). *J Ind Microbiol Biotechnol* **30:** 462–467.

Hu, H., Zhang, Q., and Ochi, K. (2002) Activation of antibiotic biosynthesis by specified mutations in the *rpoB* gene (encoding the RNA polymerase beta subunit) of *Streptomyces lividans*. *J Bacteriol* **184:** 3984–3991.

Hutchings, M.I., Hoskisson, P.A., Chandra, G., and Buttner, M.J. (2004) Sensing and responding to diverse extracellular signals? Analysis of the sensor kinases and response regulators of *Streptomyces coelicolor* A3(2). *Microbiology* **150:** 2795–2806.

Jones, G., and Dyson, P. (2006) Evolution of transmembrane protein kinases implicated in coordinating remodeling of gram-positive peptidoglycan: inside versus outside. *J Bacteriol* **188:** 7470–7476.

Julian, E., Roldan, M., Sanchez-Chardi, A., Astola, O., Agusti, G., and Luquin, M. (2010) Microscopic cords, a virulence-related characteristic of *Mycobacterium tuberculosis*, are also present in nonpathogenic mycobacteria. *J Bacteriol* **192:** 1751–1760.

Kang, C.M., Abbott, D.W., Park, S.T., Dascher, C.C., Cantley, L.C., and Husson, R.N. (2005) The *Mycobacterium tuberculosis* serine/threonine kinases PknA and PknB: substrate identification and regulation of cell shape. *Genes Dev* **19:** 1692–1704.

Kieser, T., Bibb, M.J., Buttner, M.J., Chater, K.F., and Hopwood, D.A. (2000) *Practical Streptomyces Genetics*. Norwich, UK: John Innes Foundation.

Kim, D.J., Huh, J.H., Yang, Y.Y., Kang, C.M., Lee, I.H., Hyun, C.G., *et al*. (2003) Accumulation of S-adenosyl-L-methionine enhances production of actinorhodin but inhibits sporulation in *Streptomyces lividans* TK23. *J Bacteriol* **185:** 592–600.

Kodani, S., Hudson, M.E., Durrant, M.C., Buttner, M.J., Nodwell, J.R., and Willey, J.M. (2004) The SapB morphogen is a lantibiotic-like peptide derived from the product of the developmental gene *ramS* in *Streptomyces coelicolor*. *Proc Natl Acad Sci USA* **101:** 11448–11453.

Lai, C., Xu, J., Tozawa, Y., Okamoto-Hosoya, Y., Yao, X., and Ochi, K. (2002) Genetic and physiological characterization of *rpoB* mutations that activate antibiotic production in *Streptomyces lividans*. *Microbiology* **148:** 3365–3373.

Mieczkowski, C., Iavarone, A.T., and Alber, T. (2008) Auto-activation mechanism of the *Mycobacterium tuberculosis* PknB receptor Ser/Thr kinase. *EMBO J* **27:** 3186–3197.

Mistry, B.V., Del Sol, R., Wright, C., Findlay, K., and Dyson, P. (2008) FtsW is a dispensable cell division protein required for Z-ring stabilization during sporulation septation in *Streptomyces coelicolor*. *J Bacteriol* **190:** 5555–5566.

Molle, V., and Kremer, L. (2010) Division and cell envelope regulation by Ser/Thr phosphorylation: mycobacterium shows the way. *Mol Microbiol* **75:** 1064–1077.

Nieselt, K., Battke, F., Herbig, A., Bruheim, P., Wentzel, A., Jakobsen, O.M., *et al*. (2010) The dynamic architecture of the metabolic switch in *Streptomyces coelicolor*. *BMC Genomics* **11:** 10.

O'Hare, H.M., Duran, R., Cervenansky, C., Bellinzoni, M., Wehenkel, A.M., Pritsch, O., *et al*. (2008) Regulation of glutamate metabolism by protein kinases in mycobacteria. *Mol Microbiol* **70:** 1408–1423.

Okamoto, S., Lezhava, A., Hosaka, T., Okamoto-Hosoya, Y., and Ochi, K. (2003) Enhanced expression of S-adenosylmethionine synthetase causes overproduction of actinorhodin in *Streptomyces coelicolor* A3(2). *J Bacteriol* **185:** 601–609.

Pallen, M., Chaudhuri, R., and Khan, A. (2002) Bacterial FHA domains: neglected players in the phospho-threonine signalling game? *Trends Microbiol* **10:** 556–563.

Park, S.T., Kang, C.M., and Husson, R.N. (2008) Regulation of the SigH stress response regulon by an essential protein kinase in *Mycobacterium tuberculosis*. *Proc Natl Acad Sci USA* **105:** 13105–13110.

Petrickova, K., and Petricek, M. (2003) Eukaryotic-type protein kinases in *Streptomyces coelicolor*: variations on a common theme. *Microbiology* **149:** 1609–1621.

Redenbach, M., Kieser, H.M., Denapaite, D., Eichner, A., Cullum, J., Kinashi, H., and Hopwood, D.A. (1996) A set of ordered cosmids and a detailed genetic and physical map for the 8 Mb *Streptomyces coelicolor* A3(2) chromosome. *Mol Microbiol* **21:** 77–96.

Sambrook, J., and Russell, D.W. (2001) *Molecular Cloning: A Laboratory Manual*. Cold Spring Harbor, NY, USA: Cold Spring Harbor Press.

Schultz, C., Niebisch, A., Schwaiger, A., Viets, U., Metzger, S., Bramkamp, M., and Bott, M. (2009) Genetic and biochemical analysis of the serine/threonine protein kinases PknA, PknB, PknG and PknL of *Corynebacterium glutamicum*: evidence for non-essentiality and for phosphorylation of OdhI and FtsZ by multiple kinases. *Mol Microbiol* **74:** 724–741.

Shah, I.M., Laaberki, M.H., Popham, D.L., and Dworkin, J. (2008) A eukaryotic-like Ser/Thr kinase signals bacteria to exit dormancy in response to peptidoglycan fragments. *Cell* **135:** 486–496.

Thakur, M., and Chakraborti, P.K. (2006) GTPase activity of mycobacterial FtsZ is impaired due to its transphosphorylation by the eukaryotic-type Ser/Thr kinase, PknA. *J Biol Chem* **281:** 40107–40113.

Umeyama, T., Lee, P.C., and Horinouchi, S. (2002) Protein serine/threonine kinases in signal transduction for secondary metabolism and morphogenesis in *Streptomyces*. *Appl Microbiol Biotechnol* **59:** 419–425.

Villarino, A., Duran, R., Wehenkel, A., Fernandez, P., England, P., Brodin, P., *et al*. (2005) Proteomic identification of *M. tuberculosis* protein kinase substrates: PknB recruits GarA, a FHA domain-containing protein, through activation loop-mediated interactions. *J Mol Biol* **350:** 953–963.

Viollier, P.H., Minas, W., Dale, G.E., Folcher, M., and Thompson, C.J. (2001a) Role of acid metabolism in *Streptomyces coelicolor* morphological differentiation and antibiotic biosynthesis. *J Bacteriol* **183:** 3184–3192.

Viollier, P.H., Nguyen, K.T., Minas, W., Folcher, M., Dale, G.E., and Thompson, C.J. (2001b) Roles of aconitase in growth, metabolism, and morphological differentiation of *Streptomyces coelicolor*. *J Bacteriol* **183:** 3193–3203.

Viollier, P.H., Kelemen, G.H., Dale, G.E., Nguyen, K.T., Buttner, M.J., and Thompson, C.J. (2003) Specialized osmotic stress response systems involve multiple SigB-like sigma factors in *Streptomyces coelicolor*. *Mol Microbiol* **47:** 699–714.

Wehmeier, U.F. (1995) New multifunctional *Escherichia coli-Streptomyces* shuttle vectors allowing blue-white screening on XGal plates. *Gene* **165:** 149–150.

Yanisch-Perron, C., Vieira, J., and Messing, J. (1985) Improved M13 phage cloning vectors and host strains: nucleotide sequences of the M13mp18 and pUC19 vectors. *Gene* **33:** 103–119.

Yeats, C., Finn, R.D., and Bateman, A. (2002) The PASTA domain: a beta-lactam-binding domain. *Trends Biochem Sci* **27:** 438.

Supporting information

Additional Supporting Information may be found in the online version of this article:

Fig. S1. Enriched phosphoproteomes of (A) M145, (B) *pknB* mutant and (C) *fhaAB* mutant. Cultures were grown on NE medium for 48 h and phosphoproteins subsequently enriched from cell extracts by affinity chromatography using a phosphoprotein purification kit (Qiagen). Samples were subsequently analysed by SDS-PAGE, followed by detection of phosphoproteins with Pro-Q Diamond stain.

Please note: Wiley-Blackwell are not responsible for the content or functionality of any supporting materials supplied by the authors. Any queries (other than missing material) should be directed to the corresponding author for the article.

